High nuclearity manganese(III) compounds containing phenol-pyrazole ligands: the influence of the ligand on the core geometry†

Marta Viciano-Chumillas,[a,b] Graham de Ruiter,[a] Stefania Tanase,‡[a] Jan M. M. Smits,[c] René de Gelder,[c] Ilpo Mutikainen,[d] Urho Turpeinen,[d] L. Jos de Jongh*[b] and Jan Reedijk*[a]

Received 24th November 2009, Accepted 15th January 2010
First published as an Advance Article on the web 10th February 2010
DOI: 10.1039/b924776a

Three high-nuclearity manganese(III) clusters have been synthesized and characterized: $[Mn_8(\mu_4\text{-}O)_4(phpzH)_8(thf)_4]$ (**1**), $[Mn_8(\mu_4\text{-}O)_4(phpzH)_4(EtOH)_4]\cdot 2EtOH$ (**2**), and $[Mn_6(\mu_3\text{-}O)_4(\mu_3\text{-}Br)_2(HphpzEt)_6(phpzEt)]$ (**3**). Compounds **1** and **2** contain a $[Mn_8(\mu_4\text{-}O_4)(phpzH)_8]$ core in which antiferromagnetic interactions between the manganese(III) ions are found. Compound **3** is a hexanuclear manganese(III) cluster in which weak ferromagnetic interactions appear to be operative. The formation and the stability of the cluster cores in relation to the type of phenol-pyrazole ligand and the reaction conditions are discussed.

Introduction

Polynuclear paramagnetic transition-metal compounds have attracted much attention in the last decades, because of their relevance to bioinorganic chemistry as functional models for the active sites of many metallobiomolecules[1] and also because of their magnetic properties.[2,3] The interest in the magnetic properties of these polynuclear compounds derives from their ability to act as molecule-based magnets, exhibiting a remnant magnetic moment below a critical magnetic ordering temperature. Besides the more familiar long-range magnetic ordering into a 3D magnetic lattice,[4] the magnetic remanence can also appear in the form of a 0D phenomenon, with the so-called single-molecule magnet behaviour (SMM),[2,3] in which the origin of the remnant moment is purely molecular and interesting quantum properties are associated with this type of behaviour. In the search of novel SMM's, numerous polynuclear cluster compounds have been synthesized.[2,3] Most of them are formed by manganese ions in various oxidation states stabilized by carboxylate[5,6] and/or oxime ligands.[7-9] However, the use of pyrazole ligands to obtain large polymetallic clusters is still under research and the number of polynuclear compounds containing these type of ligands, especially of high-nuclearity remains low.[10,11] For most of the polymetallic clusters containing pyrazole ligands reported so far, antiferromagnetic interactions between the metal ions are present.[10,11] Only in a few cases, predominant ferromagnetic interactions between the metal ions are found operative.[12-16] Therefore, new research in this direction is considered as highly relevant, not only to obtain novel polymetallic compounds containing new pyrazole-based ligands, but also to obtain molecular-based materials with the desired magnetic properties.

A common synthetic approach to obtain new polymetallic clusters is the modification of known molecules by introducing subtle variations, such as suitable bridging ligands, addition of solvents, *etc.* In this way, it is also easier to establish magneto-structural correlations and to modify further the molecule to achieve desired magnetic properties.

In our group, an octanuclear manganese(III) compound with formula $[Mn_8(\mu_4\text{-}O)_4(phpzMe)_8(thf)_4]$ was reported with the ligand 5(3)-(2-hydroxyphenyl)-3(5)-methylpyrazole, H_2phpzMe.[17] This octanuclear cluster contains solvent molecules at the periphery. Therefore, in this work, the study of the stability of the $[Mn_8(\mu_4\text{-}O)_4(phpzR)_8]$ core is presented investigating the effect of different solvents under comparable synthetic conditions. Furthermore, the replacement of the phenol-pyrazole ligand H_2phpzMe by other derivatives such as H_2phpzH (3(5)-(2-hydroxyphenyl)pyrazole) and H_2phpzEt (3(5)-(2-hydroxyphenyl)-5(3)-ethylpyrazole), under similar synthetic conditions was carried out to check whether the metal-core motif remains unperturbed. In this work, two new octanuclear manganese(III) compounds with the general formula $[Mn_8(\mu_4\text{-}O)_4(phpzH)_8(S)_4]$ (S = thf (**1**) and EtOH (**2**)) and one hexanuclear manganese(III) compound, $[Mn_6(\mu_3\text{-}O)_4(\mu_3\text{-}Br)_2(HphpzEt)_6(phpzEt)]$ (**3**) are reported. Temperature-dependent magnetic susceptibility studies indicate strong antiferromagnetic interactions in the octanuclear compounds **1** and **2**, whereas weak ferromagnetic interactions are found operative in compound **3**.

[a]*Gorlaeus Laboratories, Leiden Institute of Chemistry, Leiden University, P. O. Box 9502, 2300, RA, Leiden, The Netherlands. E-mail: reedijk@chem.leidenuniv.nl; Fax: +31 71 527 4671; Tel: +31 71 527 4459*
[b]*Kamerlingh Onnes Laboratory, Leiden Institute of Physics, Leiden University, P. O. Box 9504, 2300, RA, Leiden, The Netherlands. E-mail: jongh@physics.leidenuniv.nl; Fax: +31 71 527 5404; Tel: +31 71 527 5466*
[c]*Solid State Chemistry, Institute for Molecules and Materials, Radboud University Nijmegen, Heijendaalseweg 135, 6525, AJ, Nijmegen, The Netherlands*
[d]*Laboratory of Inorganic Chemistry, Department of Chemistry, University of Helsinki, P. O. Box 55 (A.I.Virtasen aukio 1), 00014, Helsinki, Finland*

† Electronic supplementary information (ESI) available: Crystallographic, structural data and figure of compound **1a**, selected bonds and angles information for compounds **2** and **3** and hydrogen bond details for compound **2**. CCDC reference numbers 676870 (**1a**), 753768 (**2**) and 753767 (**3**). For ESI and crystallographic data in CIF or other electronic format see DOI: 10.1039/b924776a

‡ Current address: van't Hoff Institute for Molecular Sciences, University of Amsterdam, Nieuwe Achtergracht 166, 1018 WV Amsterdam, The Netherlands

Experimental

General remarks

Starting materials and the ligand 3(5)-(2-hydroxyphenyl)pyrazole (H_2phpzH) were purchased from Aldrich. All manipulations were performed using materials as received. The ligand 3(5)-(2-hydroxyphenyl)-5(3)-ethylpyrazole (H_2phpzEt) has been synthesized according to the reported procedure.[18] **Caution!** Perchlorate salts are potentially explosive. Such compounds should be used in small quantities and should be treated with utmost care at all times.

Synthesis

$[Mn_8(\mu_4\text{-}O)_4(phpzH)_8(thf)_4]$ (1). The reaction of $Mn(ClO_4)_2\cdot 6H_2O$ (102 mg, 0.28 mmol) in tetrahydrofuran (THF) with H_2phpzH (91 mg, 0.56 mmol) in THF in the presence of triethylamine (1.12 mmol) affords a dark brown solid (53 mg, 0.026 mmol). Yield: 74%. Slow evaporation of the reaction mixture affords brown crystals. The poor quality of the crystal (**1a**) reveals a missing tetrahydrofuran molecule agreeing with the formula $[Mn_8(\mu_4\text{-}O)_4(phpzH)_8(thf)_3]$ (**1a**). Anal. calcd for **1** *i.e.* with 4 thf ($C_{88}H_{80}Mn_8N_{16}O_{16}$): C 51.38, H 3.92, N 10.89. Found: C 51.92, H 4.51, N 10.60. IR (ν_{max}/cm^{-1}: 1600 (m), 1564 (m), 1477 (vs), 1456 (s), 1436 (m), 1340 (m), 1295 (s), 1234 (s), 1136 (s), 1080 (s), 1036 (m), 980 (m), 860 (s), 845 (s), 753 (vs), 668 (vs), 648 (s), 623 (vs), 584 (vs), 563 (vs), 443 (vs).

$[Mn_8(\mu_4\text{-}O)_4(phpzH)_4(EtOH)_4]\cdot 2EtOH$ (2). The reaction of $Mn(ClO_4)_2\cdot 4H_2O$ (102 mg, 0.28 mmol) in ethanol with a solution of H_2phpzH (90 mg, 0.56 mmol) and triethylamine (1.12 mmol) in ethanol provides brown crystals (28 mg, 0.015 mmol) that were collected by filtration, washed with Et_2O and dried in vacuum. Compound **2** was found to exchange the ethanol terminal ligands by water molecules upon air exposure, to form $[Mn_8(\mu_4\text{-}O)_4(phpzH)_4(H_2O)_4]\cdot H_2O$ (**2a**). Yield: 43%. Anal. calcd for **2a** ($C_{72}H_{58}Mn_8N_{16}O_{17}$): C 46.52, H 3.12, N 12.06. Found: C 46.79, H 2.85, N 11.98. IR (ν_{max}/cm^{-1}: 3054 (vw), 2988 (vw), 1600 (s), 1564 (m), 1558 (m), 1516 (m), 1480 (vs), 1456 (s), 1436 (s), 1338 (s), 1293 (s), 1249 (s), 1232 (vs), 1216 (s), 1133 (vs), 1079 (s), 1036 (m), 980 (m), 943 (w), 862 (s), 844 (s), 782 (m), 747 (vs), 677 (vs), 668 (vs), 650 (s), 618 (vs), 586 (vs), 561 (vs), 436 (s), 384 (s), 358 (s), 328 (s), 306 (s).

$[Mn_6(\mu_3\text{-}O)_4(\mu_3\text{-}Br)_2(HphpzEt)_6(phpzEt)]$ (3). The reaction of $MnBr_2\cdot 4H_2O$ (86 mg, 0.3 mmol) with H_2phpzEt (56 mg, 0.3 mmol) in the presence of triethylamine (0.45 mmol) in CH_3CN, resulted in the formation of a dark brown crystalline precipitate (49 mg, 0.026 mmol). Yield: 53%. Crystals suitable for X-ray crystallography were obtained by diffusion of hexane into a dichloromethane solution of **3**. Anal. calcd for $[Mn_6(\mu_3\text{-}O)_4(\mu_3\text{-}Br)_2(HphpzEt)_6(phpzEt)]$ (**3**) ($C_{77}H_{76}Br_2Mn_6N_{14}O_{11}$): C 49.64, H 4.11, N 10.53. Found: C 49.29, H 4.27, N 10.7. IR (ν_{max}/cm^{-1}: 3242 (w), 2972 (w), 1600 (s), 1568 (m), 1558 (s), 1532 (w), 1506 (w), 1480 (s), 1464 (s), 1448 (vs), 1409 (w), 1337 (m), 1306 (s), 1282 (s), 1268 (s), 1250 (vs), 1194 (w), 1120 (vs), 1053 (w), 1036 (m), 990 (m), 934 (w), 860 (s), 805 (m), 748 (vs), 712 (s), 668 (vs), 614 (s), 586 (s), 565 (s), 442 (w), 424 (w), 415 (w), 384 (w), 366 (m), 352 (w), 311 (w).

Physical measurements

Elemental analyses for C, H and N were performed on a Perkin-Elmer 2400 series II analyzer. Infrared spectra (4000–300 cm^{-1}) were recorded on a Perkin-Elmer Paragon 1000 FTIR spectrometer equipped with a Golden Gate ATR device, using the reflectance technique. Thermogravimetric analysis was carried out on a Mettler Toledo TGS/SDTA851e in the temperature range 25 to 250 °C. DC and AC magnetic data were recorded using a Quantum Design MPMS-5 SQUID susceptometer. The magnetic susceptibilities were measured from 1.8 to 300 K on polycrystalline samples in a gelatine capsule with an applied field of 0.1 T. The magnetization was measured from 2 up to 20 K in the 0–5 T range. Data were corrected for magnetization of the sample holder and for diamagnetic contributions, which were estimated from Pascal's constants.[4]

X-Ray crystallography

Intensity data for single crystals of **1a**, **2** and **3** were collected using Mo Kα radiation ($\lambda = 0.71073$ Å) on a Nonius KappaCCD diffractometer. Crystal and refinement data for **1a** is collected in the ESI,† whereas for **2** and **3** are collected in Table 1. The intensity data were corrected for Lorentz and polarization effects, and for absorption (multi-scan absorption correction[19]). The structures were solved by Patterson methods.[20] The programs EvalCCD,[21,22] DIRDIF96,[23] SHELXS-97[24] and SHELXL-97[25] were used for data reduction, structure solution and refinement, respectively. All non-hydrogen atoms were refined with anisotropic displacement parameters. Compound **3** contains disordered solvent molecules, being three CH_2Cl_2 each with population 0.5 and eight water molecules with population parameters from 0.5 to 0.3333. CCDC-676870 (**1a**), CCDC-753768 (**2**) and CCDC-753767 (**3**) contain the supplementary crystallographic data for this paper. Geometric calculations and molecular graphics were performed with the PLATON package.[26]

Results and discussion

Synthesis

The reaction of $Mn(ClO_4)_2\cdot 6H_2O$ with H_2phpzH in tetrahydrofuran in the ratio 1 : 2, or 1 : 1 and in the presence of triethylamine as base yielded the compound **1**, which is of similar geometry as the cluster $[Mn_8(\mu_4\text{-}O)_4(phpzMe)_8(thf)_4]$ reported previously.[17] The same reaction in ethanol affords compound **2**. As shown below, these octanuclear manganese(III) compounds contain a stable core, where the main difference arises from the different solvent used in the reaction. The addition of an excess of triethylamine to a solution of mononuclear compounds with the general formula $[Mn(HphpzR)_2X]$ (R = H, Me, $X^- = Cl^-$, Br^-)[27] affords also complexes containing the core $[Mn_8(\mu_4\text{-}O)_4(phpzR)_8]$. The formation of the octanuclear compounds $[Mn_8(\mu_4\text{-}O)_4(phpzR)_8]$ (R = H, Me) can be avoided by using more bulky ligands, such as H_2phpzEt. For example the hexanuclear compound **3** is formed in the presence of triethylamine as base and acetonitrile as solvent. The amount of base is paramount, since it leads to the formation of mononuclear manganese(III) complexes,[27] or higher nuclearity manganese(III) complexes, such as compounds **1–3**.

Table 1 Crystal data and structure refinements details for compounds **2** and **3**

	2	**3**
Formula	$C_{80}H_{72}Mn_8N_{16}O_{16},2(C_2H_6O)$	$C_{77}H_{76}Br_2Mn_6N_{14}O_{11}\cdot0.5(CH_2Cl_2O),CH_2Cl_2O_3$
Formula weight/g mol^{-1}	2045.20	2046.19
Crystal system	Triclinic	Monoclinic
Space group	$P\bar{1}$	$P2_1/c$
a/Å	15.284(3)	14.589(2)
b/Å	15.918(3)	28.014(4)
c/Å	18.924(3)	24.429(4)
α/°	82.82(3)	90
β/°	69.50(3)	103.478(16)
γ/°	84.94(3)	90
V/Å^3	4273.8(16)	9709(3)
Z	2	4
D_{calcd}/g cm^{-3}	1.589	1.400
Crystal size	0.04 × 0.08 × 0.20	0.05 × 0.15 × 0.18
Number of collected reflections (unique)	60 496 (16 578)	133 876 (19 030)
Number of observed reflections [$I_o > 2\sigma(I_o)$]	11 208	13 305
Internal R factor	0.068	0.065
Number of parameters	1173	1120
Goodness-of-fit S on F^2	1.06	1.09
Largest peak and hole in final difference Fourier map/e Å^{-3}	0.67 and –0.75	1.26 and –0.50
μ/mm^{-1}	1.220	1.724
R_1 [a][$I > 2.0\sigma(I)$]	0.0463	0.0580
wR_2 [b][all data]	0.1011	0.1595
T/K	173	173

[a] $R_1 = \sum\|F_o\| - |F_c\|/\sum|F_o|$. [b] $wR_2 = \{\sum[w(F_o^2 - F_c^2)^2]/\sum w(F_o^2)^2\}^{1/2}$.

Repeated elemental analyses of compound **2** show that the solvent molecules are substituted by water molecules upon air exposure to form $[Mn_8(\mu_4\text{-}O)_4(phpzH)_8(H_2O)_4]\cdot H_2O$ (**2a**). Thermogravimetric analysis (TGA) of **2a** was performed by heating up the sample to 250 °C; a mass loss of *ca.* 5% has been observed, in agreement with the presence of five water molecules.

Description of the molecular structures

Crystal and refinement data are shown in Table S1 (ESI)† for compound **1a** and in Table 1 for compounds **2** and **3**. Compounds **1a** and **2** crystallize in the triclinic space group $P\bar{1}$. Both structures comprise eight manganese(III) ions, four of them are bound through oxide ligand bridges in a distorted cubane geometry, as shown in Fig. 1 for compound **2**. The other four manganese(III) ions are at the periphery with eight doubly deprotonated $phpzH^{2-}$ ligands and solvent molecules, tetrahydrofuran and ethanol for compounds **1a** and **2**, respectively. The relatively poor quality of the crystal (**1a**) of compound **1** reveals a missing tetrahydrofuran molecule, considering the elemental analysis performed and the analogy with the related cluster $[Mn_8(\mu_4\text{-}O)_4(phpzMe)_8(thf)_4]$, reported previously.[17] Therefore only three tetrahydrofuran molecules are present in compound **1a**. More detailed crystallographic data for compounds **1a–3** are given in the ESI.†

Compound **2**, $[Mn_8(\mu_4\text{-}O)_4(phpzH)_8(EtOH)_4]\cdot 2EtOH$, contains four coordinated ethanol molecules and two ethanol molecules of crystallization, stabilized by hydrogen bonding interactions in the lattice (Fig. 1). The Mn–$O_{solvent}$ distances are larger in **2** (av. 2.33 Å) than in **1a** (av. 2.28 Å). As a result of the weak Mn–$O_{solvent}$ bonds in **2**, the crystallinity is partially lost, upon removing the crystals from the mother liquid, as confirmed by the elemental analysis and the TGA analysis. The closest Mn···Mn bond distances are in the range of 3.175(3)–3.434(3) Å and 3.2209(10)–3.4626(10) Å for compounds **1a** and **2**, respectively. Selected angles for the compound $[Mn_8(\mu_4\text{-}O)_4(phpzH)_8(EtOH)_4]\cdot 2EtOH$ (**2**) are shown in Table 2. The Jahn–Teller axes involve the solvent molecules (tetrahydrofuran or ethanol) coordinated to the peripheral manganese(III) ions. Considering the distortion of compounds **1a** and **2**, the Jahn–Teller axes are arranged in two main directions that are "perpendicular" to each other, with the same number of Jahn–Teller axes in the "same direction" for the manganese(III) ions that are at the periphery and in the cubane

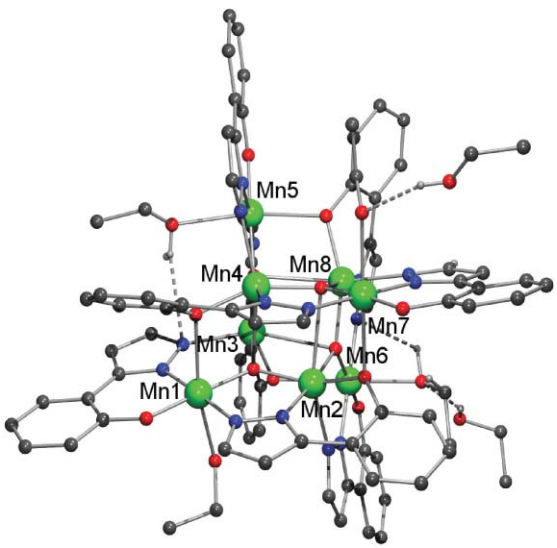

Fig. 1 Platon projection of the compound **2**. Hydrogen atoms that are not involved in hydrogen bonding interactions are omitted for clarity. Colour code: green = manganese; blue = nitrogen; red = oxygen; grey = carbon.

Table 2 Selected bond lengths (Å) and angles (°) for the compound **2**

Bond lengths/Å			
Mn(1)···Mn(2)	3.3967(11)	Mn(1)···Mn(3)	3.3034(10)
Mn(1)···Mn(4)	3.4626(10)	Mn(2)···Mn(6)	3.3296(10)
Mn(2)···Mn(7)	3.4578(10)	Mn(3)···Mn(5)	3.3700(10)
Mn(3)···Mn(6)	3.4092(11)	Mn(4)···Mn(5)	3.3203(11)
Mn(4)···Mn(7)	3.3672(11)	Mn(5)···Mn(8)	3.4355(11)
Mn(6)···Mn(8)	3.3896(10)	Mn(7)···Mn(8)	3.3446(10)
Mn(2)···Mn(3)	3.2352(11)	Mn(2)···Mn(4)	3.2209(10)
Mn(2)···Mn(8)	3.2385(10)	Mn(3)···Mn(4)	3.2387(10)
Mn(3)···Mn(8)	3.2221(10)	Mn(4)···Mn(8)	3.2633(10)
Bond angles/°			
Mn(1)–O(1)–Mn(2)	125.19(14)	Mn(1)–O(1)–Mn(3)	119.49(15)
Mn(1)–O(1)–Mn(4)	96.89(10)	Mn(2)–O(1)–Mn(3)	115.21(13)
Mn(2)–O(1)–Mn(4)	87.64(10)	Mn(3)–O(1)–Mn(4)	88.32(10)
Mn(2)–O(2)–Mn(4)	86.29(10)	Mn(2)–O(2)–Mn(7)	95.61(11)
Mn(2)–O(2)–Mn(8)	86.71(10)	Mn(4)–O(2)–Mn(7)	123.32(14)
Mn(4)–O(2)–Mn(8)	115.33(14)	Mn(7)–O(2)–Mn(8)	121.33(14)
Mn(3)–O(3)–Mn(4)	115.51(13)	Mn(3)–O(3)–Mn(5)	123.62(14)
Mn(3)–O(3)–Mn(8)	87.78(10)	Mn(4)–O(3)–Mn(5)	120.74(14)
Mn(4)–O(3)–Mn(8)	89.36(11)	Mn(5)–O(3)–Mn(8)	95.99(10)
Mn(2)–O(4)–Mn(3)	87.49(10)	Mn(2)–O(4)–Mn(6)	120.41(13)
Mn(2)–O(4)–Mn(8)	115.27(12)	Mn(3)–O(4)–Mn(6)	93.92(11)
Mn(3)–O(4)–Mn(8)	87.08(10)	Mn(6)–O(4)–Mn(8)	124.30(13)

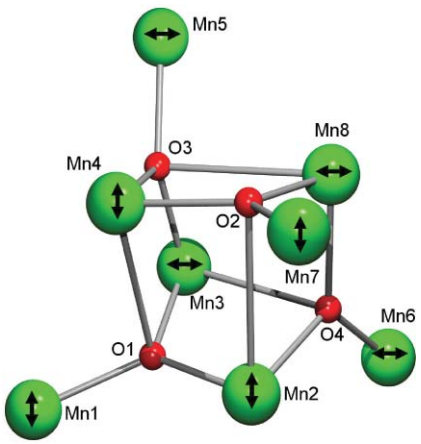

Fig. 2 The $[Mn_8(\mu_4\text{-}O)_4]^{16+}$ core of compound **2** showing the orientation of the Jahn–Teller axes (↔).

core (Fig. 2 (**2**) and Fig. S1 (**1a**)).† In compound **2**, hydrogen bonding is present between the lattice ethanol molecules and the coordinated ethanol molecules (ESI, Table S4).†

Compound **3** crystallizes in the monoclinic space group $P2_1/c$. As shown in Fig. 3, compound **3** consists of a hexanuclear manganese(III) compound with a $[Mn_6(\mu_3\text{-}O)_4(\mu_3\text{-}Br)_2]^{8+}$ core. At the periphery, six $HphpzEt^-$ ligands are present in a bidentate chelating mode and one $phpzEt^{2-}$ ligand is bridging two manganese(III) ions, Mn(4) and Mn(5). The $[Mn_6(\mu_3\text{-}O)_4(\mu_3\text{-}Br)_2]^{8+}$ core can be described as an octahedron in which the manganese(III) ions are in the vertices (Fig. 4). Mn(2), Mn(3), Mn(4) and Mn(6) form the equatorial plane of the octahedron, whereas Mn(1) and Mn(5) are at the axial positions. Another possible description for **3** is as an inverted adamantane, $[Mn_6O_4]$, since the Mn/O ratio is inverted with regard to the commonly observed value for the adamantane subunit, $[Mn_4O_6]$.[28] The octahedron is comprised of four faces in which the manganese(III) ions are bridged by μ_3-oxide

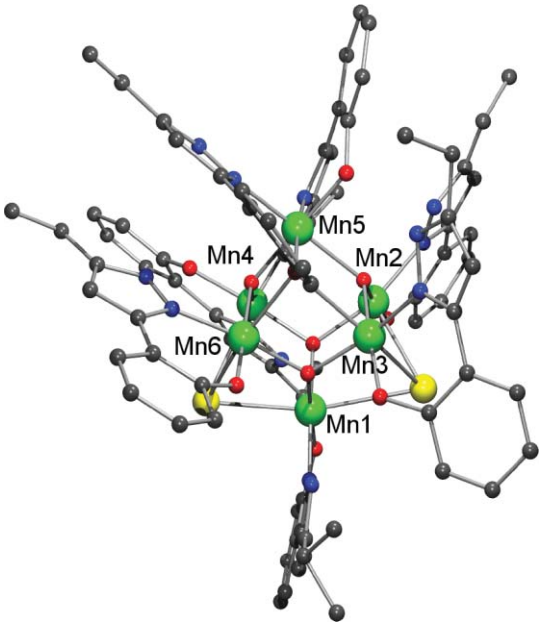

Fig. 3 Platon projection of the compound $[Mn_6(\mu_3\text{-}O)_4(\mu_3\text{-}Br)_2(HphpzEt)_6(phpzEt)]$ (**3**). Hydrogen atoms are omitted for clarity. Colour code: green = manganese; yellow = bromide; blue = nitrogen; red = oxygen; grey = carbon.

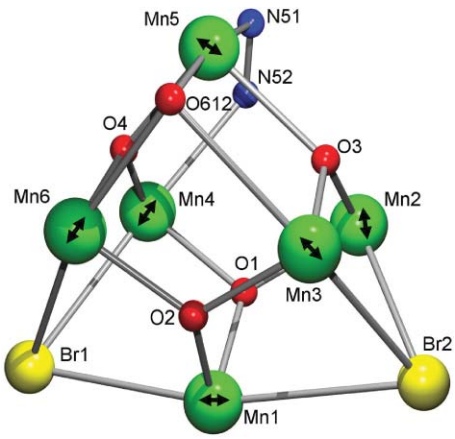

Fig. 4 The $[Mn_6(\mu_3\text{-}O)_4(\mu_3\text{-}O_{(phpzEt)})(\mu_3\text{-}Br)_2]^{8+}$ core of compound **3**, showing the Mn_6 octahedral geometry and the Jahn–Teller axes (↔).

ligands, two faces are bridged by the μ_3-bromide ligand, one face is bridged by a μ-phenolato oxygen of one of the $HphpzEt^-$ ligand and one face contains a $phpzEt^{2-}$ ligand, in which the pyrazolato ligand bridges Mn(4) and Mn(5). Selected bond distances and angles are listed in Table 3 and more detailed crystallographic information is provided in the ESI.† The Mn–Br bond lengths are in the range of 2.731–3.008 Å. The manganese(III) ions are in an very distorted octahedral geometry. The Jahn–Teller distortion involves the bromide ions, except for Mn(5), which is formed by O(3)–Mn(5)–N(61), where O(3) is an μ_3-oxide ligand and N(61) is a nitrogen from the pyrazole ring of the $HphpzEt^-$ ligand (Fig. 4). The angles spanned by the atoms that form the Jahn–Teller axes have values ranging between 154.42–167.87°. The $Mn–O_{eq}$ distances are in the range of 1.863 to 1.994 Å, whereas the $Mn–N_{eq}$ distances are between 1.975–2.035 Å. The smallest Mn···Mn intercluster distance is 8.182 Å. Disordered

Table 3 Selected bond lengths (Å) and angles (°) for the complex $[Mn_6(\mu_3\text{-}O)_4(\mu_3\text{-}Br)_2(HphpzEt)_6(phpzEt)]$ (**3**)

Bond lengths/Å							
Mn(1)–O(2)	1.876(3)	Mn(1)–O(1)	1.901(3)	Mn(1)–Br(1)	2.7488(10)	Mn(1)–Br(2)	3.0076(10)
Mn(2)–O(3)	1.878(3)	Mn(2)–O(1)	1.924(3)	Mn(2)–Br(2)	2.814(4)	Mn(3)–O(3)	1.863(3)
Mn(3)–O(2)	1.905(3)	Mn(3)–Br(2)	2.7353(11)	Mn(3)–O(612)	2.577(3)	Mn(4)–O(1)	1.898(3)
Mn(4)–O(4)	1.903(3)	Mn(4)–N(52)	2.260(4)	Mn(4)–Br(1)	2.9014(11)	Mn(5)–O(4)	1.901(3)
Mn(5)–O(612)	1.994(3)	Mn(5)–O(3)	2.158(3)	Mn(5)–N(61)	2.221(4)	Mn(6)–O(2)	1.910(3)
Mn(6)–O(4)	1.916(3)	Mn(6)–Br(1)	2.8517(11)	Mn(6)–O(612)	2.294(3)	Mn(1)···Mn(2)	3.2502(12)
Mn(1)···Mn(4)	3.2392(13)	Mn(1)···Mn(6)	3.2284(13)	Mn(2)···Mn(3)	3.1708(12)	Mn(2)···Mn(4)	3.2251(11)
Mn(2)···Mn(5)	3.4701(13)	Mn(3)···Mn(5)	3.2883(13)	Mn(3)···Mn(6)	3.2207(11)	Mn(5)···Mn(6)	3.0572(12)
Bond angles/°							
Mn(1)–Br(1)–Mn(4)	69.90(3)	Mn(1)–Br(1)–Mn(6)	70.37(3)	Mn(4)–Br(1)–Mn(6)	70.13(3)		
Mn(2)–Br(2)–Mn(3)	70.92(3)	Mn(1)–O(1)–Mn(2)	116.37(16)	Mn(1)–O(1)–Mn(4)	117.01(16)		
Mn(2)–O(1)–Mn(4)	115.07(17)	Mn(1)–O(2)–Mn(3)	118.19(17)	Mn(1)–O(2)–Mn(6)	117.01(16)		
Mn(3)–O(2)–Mn(6)	115.21(17)	Mn(2)–O(3)–Mn(3)	115.89(18)	Mn(2)–O(3)–Mn(5)	118.40(16)		
Mn(3)–O(3)–Mn(5)	109.49(15)	Mn(4)–O(4)–Mn(5)	122.04(17)	Mn(4)–O(4)–Mn(6)	119.87(18)		
Mn(5)–O(4)–Mn(6)	106.46(15)						

dichloromethane and water molecules are present in the crystal lattice as a result of the recrystallization process of compound **3**.

Magnetic properties

Magnetic susceptibilities were measured for compounds **1–3** as a function of temperature under a 0.1 T applied field in the range 1.8–300 K. The $\chi_M T$ product at 300 K amounts to 19.49 $cm^3\ mol^{-1}$ K and 19.45 $cm^3\ mol^{-1}$ K for compounds **1** and **2a**, respectively (as shown in Fig. 5). These values are substantially lower than expected for eight non-interacting manganese(III) ions with $g = 2.00$ (24 $cm^3\ mol^{-1}$ K), which indicates the presence of strong antiferromagnetic interactions between the eight manganese(III) ions even at room temperature. Indeed, the $\chi_M T$ value gradually decreases to 0.37 $cm^3\ mol^{-1}$ K at 2 K and 1.04 $cm^3\ mol^{-1}$ K at 4.3 K for compounds **1** and **2a**, respectively, suggesting a ground state $S_T = 0$ with low-lying excited levels. In fact, the χ_M curve presents a maximum at *ca.* 29 K for both compounds. Field dependence of the magnetization was measured at 2 K (Inset of Fig. 5). The values at 5 T are 1.82 and 2.08$N\beta$ for compounds **1** and **2a**, respectively. In both cases, the values are far below the saturation limit of 32$N\beta$ for eight non-interacting manganese(III) ions, confirming the presence of strong antiferromagnetic interactions between the manganese(III) ions.

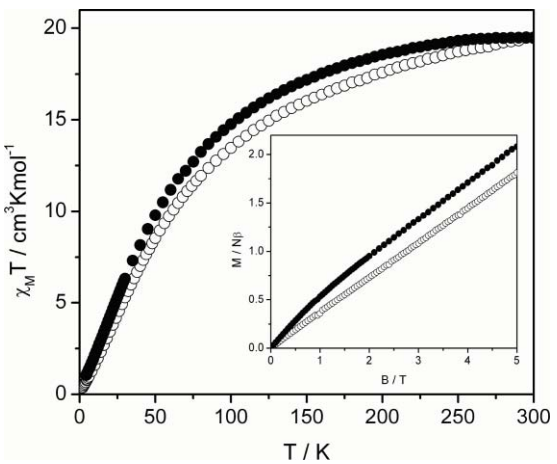

Fig. 5 Plot of $\chi_M T$ *vs.* T in the range 4 to 300 K in 0.1 T applied field for $[Mn_8(\mu_4\text{-}O)_4(phpzH)_4(thf)_4]$ (**1**) (○) and $[Mn_8(\mu_4\text{-}O)_4(phpzH)_4]\cdot 5H_2O$ (**2a**) (●). Inset, field dependence of the magnetization at 2 K.

Compounds **1a** and **2** contain four manganese(III) ions in a distorted cubane core, $[Mn_4O_4]$ and four manganese(III) ions at the periphery. Because of the low symmetry of the cluster geometry, it is not possible to apply the Kambe vector-coupling method to evaluate the magnetic exchange interactions. Although several other octanuclear manganese(III) compounds have been reported in the literature,[28–38] none of them contains the same structural topology. One type of octanuclear manganese(III) compounds consists of two linked tetranuclear subunits,[31,32,34,35,38] in which antiferromagnetic interactions between the manganese(III) ions in the subunits are observed and rather weak antiferromagnetic interactions between these subunits are found.[31,32,35,38] In other compounds with different topologies, antiferromagnetic interactions resulting in a high-spin ground state,[29] or even ferromagnetic interactions are observed between the manganese(III) ions.[28,30,36,37] In most of these reported compounds, the magnetic exchange interactions can be modelled on the basis of the alignment of the Jahn–Teller axes and the spin frustration present in the $[Mn_4O_2]^{8+}$ butterfly core.[28-33,35–38] On the other hand, two iron(III) compounds have been reported with the same core structure, $[Fe^{III}{}_8O_4]^{4+}$, as observed here for compounds **1a** and **2**. In that cases, pyrazole[39,40] or salicylaldoxime[41,42] are the capping ligands, and strong antiferromagnetic interactions are found between the iron(III) ions in the cubane core with those in the periphery.[39–42] In compounds **1a** and **2**, the Jahn–Teller axes are in two main directions that are nearly perpendicular to each other, considering the distortion of the cubane core (Fig. 2 and S1b in the ESI).† From this point of view, the number of Jahn–Teller axes in the same direction is equal for the manganese(III) ions in the cubane core and for those at the periphery. In addition, the manganese(III) ions in the periphery form two large Mn–O–Mn angles of values in the range of 119–125° (compound **2**) and one Mn–O–Mn angle around 93° (compound **1a**) and one Mn–O–Mn

angle around 96° (compound **2**) with the manganese(III) ions in the core (see Table 2 for compound **2**). The strength and the sign of the magnetic exchange interaction is known to be dependent on the metal–ligand–metal angle, with the strongest antiferromagnetic interactions when the metal–ligand–metal angle has a value of about 180° and weak ferromagnetic interactions at angles around 90°.[43] In compounds **1a** and **2**, the values of the Mn–O–Mn angles are appreciable larger than 90°, therefore strong antiferromagnetic interactions are expected between the manganese(III) ions. Also, the directions of the Jahn–Teller axes favours the antiferromagnetic interactions, since the spins can cancel each other and no spin canting is involved.[4]

For compound **3**, the $\chi_M T$ value of approximately 20.13 cm^3 K mol^{-1} at 300 K is higher than 18 cm^3 K mol^{-1}, the value expected for six non-interacting manganese(III) ions (Fig. 6). When lowering the temperature, the $\chi_M T$ value increases gradually to about 27 cm^3 K mol^{-1} at 16 K, then raises more steeply to about 30 cm^3 K mol^{-1} at 2.7 K, probably due to the anisotropy of the sample, followed by a final decrease that can be attributed to zero-field splitting and/or weak intermolecular interactions. The initial increase of the $\chi_M T$ curve is attributed to the presence of predominant ferromagnetic interactions between the manganese(III) ions. The values reached by $\chi_M T$ below 20 K are close to the value of 28 cm^3 K mol^{-1} corresponding to a ground state of $S_T = 7$ with $g = 2$. The magnetic susceptibility data above 100 K were fitted to the Curie–Weiss law, with $C = 18.85$ cm^3 K mol^{-1} and $\theta = +18.65$ K. The Curie constant C is in agreement with six paramagnetic manganese(III) ions with $S = 2$ and $g = 2.04$, while the positive value of the Curie–Weiss temperature θ indicates dominant albeit weak ferromagnetic interactions. From the mean-field equation, $\theta = 2zJ_{eff}S(S + 1)/3$, the effective intracluster magnetic interaction is estimated at $J_{eff} \approx 1.16$ K, assuming a number $z = 4$ of nearest neighbours in view of the molecular structure described above.

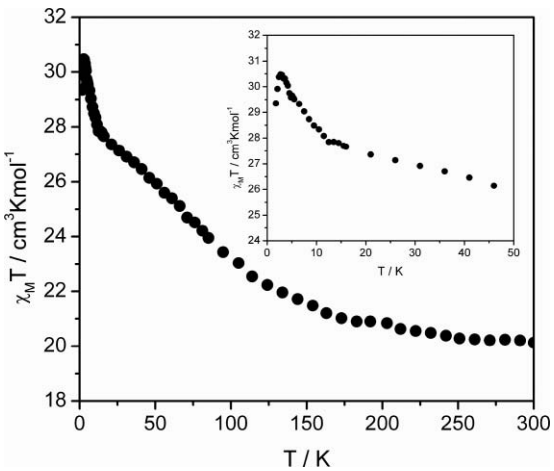

Fig. 6 Plot of $\chi_M T$ *vs.* T for **3** in the range 2 to 300 K in 0.1 T applied field. Inset, plot of $\chi_M T$ *vs.* T in the range 2 to 50 K.

Field-dependent magnetization studies were carried out below 20 K. The molar magnetization of compound **3** reaches a value of about $12N\beta$ at 5 T at 2 K as shown in Fig. 7. For six non-interacting manganese(III) ions the saturation value should be $24N\beta$. The magnetization at 2 K shows an initial fast increase, reaching a value

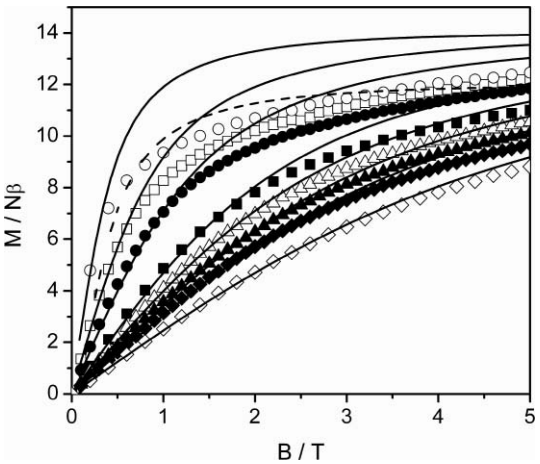

Fig. 7 Field dependence of the magnetization for compound **3** measured at 2 (○), 4 (□), 6 (●), 10 (■), 12 (△), 14 (▲), 16 (♦) and 20 (◇) K. Solid curves are the Brillouin functions calculated for $S = 2$ and $g = 2$ at the same temperatures. Dashed curve is the prediction at $T = 2$ K with an anisotropy field incorporated in the argument.

of $10N\beta$ at 1 T, not far below the $14N\beta$ corresponding to $S_T = 7$, *i.e.* to the net cluster spin indicated by the $\chi_M T$ product at lowest temperature. This value of $14N\beta$ is also obviously still far below the saturation limit of $24N\beta$. These results can be understood in terms of the weakness of the exchange interactions in combination with the strong crystal field anisotropy of the manganese(III) ions. When the intramolecular magnetic interactions are weak, the direction of the moments of the manganese(III) ions in the cluster will be dictated by their local site symmetry rather than by the magnetic exchange, *i.e.* the direction of each moment will be (at least to large extent) along its individual local Jahn–Teller axis. Since the Jahn–Teller axes for the different sites are at large angles to one another, this results in a canted magnetic structure for this cluster yielding an apparent effective net moment of about $S_T = 7N\beta$. Since the interactions are ferromagnetic, this net moment is relatively easily saturated in a field of few Tesla, where after the remaining magnetic response in higher fields will be due to the sum of the magnetic responses of the individual manganese(III) ions. For higher fields therefore, the Zeeman energy of the applied field is just competing with the single-ion anisotropy energies of the individual ions. Obviously, the field range needed to align the moments completely parallel to the field is not attained in the experiment. Indeed, as shown in Fig. 7, in the range 10–20 K the experimental $M(B)$ curves are rather close to the predictions from the Brillouin function for a single spin $S_T = 7$ at the same temperatures (solid lines). Below about 12 K the experiments fall increasingly below these predictions, which can be attributed to the single-ion anisotropy. To substantiate these assumptions, a very rough estimation of the (average) anisotropy can be obtained by adding an anisotropic field, $B_A = 2DS/g\beta$ to the applied field in the argument of the Brillouin function, resulting in the dashed line for $T = 2$ K. This clearly gives a closer fit to the experiment and yields an estimated D value of –4 cm^{-1}, which is in the range commonly observed for other manganese(III) ions in low site symmetry.[44] The corresponding anisotropy field is obtained as $B_A \approx 12$ T, far above our experimental limit indeed. Obviously, since powder data are involved, this result can only be interpreted as a qualitative explanation of the experiment.

AC magnetic susceptibility measurements were carried out in the range 2–10 K in zero DC field at different frequencies (1–10^3 Hz) and in varying DC fields (0–0.1 T) at a frequency of 99 Hz. No maximum in the susceptibility was detected down to 2 K; the susceptibility keeps increasing continuously down to the lowest temperature with no clear indication of a dependence on frequency or applied DC field. Apparently, the magnetic interactions are too weak to lead to single-molecule magnetic behaviour above 2 K.

As mentioned above, compound **3** can be described as an octahedron with the manganese(III) ions at the vertices. The Hamiltonian developed for such a system,[45] considering only two types of magnetic interactions depending on the distances between the manganese(III) ions in the octahedron, cannot be applied to this compound due to the lower symmetry of the cluster core in which several magnetic paths should be considered. However, some considerations based on the literature can be of interest to understand better the magnetic behaviour of compound **3**.

Only few hexanuclear manganese(III) clusters are known in the literature,[28,45–48] apart from the extended family of compounds with the general formula, $[Mn_6O_2(R\text{-sao})_6(X)_2(solvent)_{4\text{-}6}]$ with salicyladoxime derivative ligands (R-sao), synthesized mainly by Brechin *et al.*[7,49–52] Some of the hexanuclear manganese(III) compounds reported show dominant antiferromagnetic interactions between the manganese(III) ions, resulting in a zero- or low-spin magnetic ground state.[28,32,47,48] The compounds $[Mn_6O_4X_4(Rdbm)_6]$ ($X^- = Cl^-$, Br^-, dbm^- = dibenzoylmethane anion and R = Me, Et) present dominant ferromagnetic interactions with a total ground state of $S_T = 12$.[45,46] In the group of compounds with salicylaldoxamine ligands, antiferromagnetic and ferromagnetic interactions can be observed between the manganese(III) ions, leading to different total ground states between $4 \leq S_T \leq 12$. The type of magnetic exchange interactions has been ascribed mainly to the angle of the oxime ligand. Thus, a large distortion of the Mn–N–O–Mn angle ($\alpha > 31.3°$) can result in ferromagnetic interactions between the manganese(III) ions. As previously pointed out for other compounds, two main parameters should be considered to analyze the ferromagnetic interactions present between the manganese(III) ions, *i.e.* the Jahn–Teller axes that are the single-ion manganese(III) anisotropy axes and the Mn–O–Mn angles. In compound **3**, five of the Jahn–Teller axes intersect at bromide ions. Mn(2), Mn(3), Mn(4) and Mn(6) are similar with a bromide donor atom and a N or O donor atom defining the Jahn–Teller axes, whilst in Mn(1) such axes are defined by the two bromide atoms. The Mn–Br bond distances are long, so the magnetic interaction through them must be weak. Then, the dominant superexchange magnetic path must be through the oxido bridges. Previously, it has been observed in oxide-centred manganese(III) triangles that a distortion of the Mn–O–Mn angle towards values lower than the value of 120° for an equilateral triangle gives rise to a ferromagnetic interaction.[53–55] In compound **3** four faces of the octahedron contain such triangles, in which O(1), O(2), O(3) and O(4) are the oxido centres that bridge the three manganese(III) ions. The Mn–O–Mn angles vary from 106–122° and might be responsible for some ferromagnetic interactions between the manganese(III) ions. In addition, because of the low symmetry of the compound resulting in Jahn–Teller axes with different directions, substantial spin-canting could be present. In view of all these interviewing factors, it is difficult to arrive at a reliable prediction for the precise molecular magnetic structure.

Conclusions

High-nuclearity manganese(III) compounds have been synthesized and characterized, *i.e.* two octanuclear manganese(III) compounds with the general formula $[Mn_8(\mu_4\text{-}O)_4(phpzH)_8(S)_4]$ (S = thf (**1**) and EtOH (**2**)) and one hexanuclear, $[Mn_6(\mu_3\text{-}O)_4(\mu_3\text{-}Br)_2(HphpzEt)_6(phpzEt)]$ (**3**). The influence of different solvents on the stability of the $[Mn_8(\mu_4\text{-}O)_4(phpzR)_8]$ core has been studied. Strong antiferromagnetic interactions between the manganese(III) ions are present, leading to a ground state $S_T = 0$ for compounds **1** and **2a**. The variation of the substituents in the 5-position of the pyrazole ring, from proton and methyl to an ethyl group, indicate that the $[Mn_8(\mu_4\text{-}O)_4(phpzR)_8]$ core is not retained, probably due to the steric hindrance imposed by the ethyl group. Instead, a hexanuclear compound is obtained, *i.e.* compound **3**. In this compound, weak ferromagnetic interactions are found operative between the manganese(III) ions, leading to an effective net moment of $S_T = 7$ for the cluster. Compound **3** is one of the few examples of transition-metal ion clusters containing pyrazole ligands with dominant ferromagnetic interactions.

Acknowledgements

This work was financially supported the EC-RTN "QuEMolNa" (no. MRTN-CT-2003-504880) and the EC Network of Excellence "MAGMANet" (no. 515767-2). S. T. acknowledges the Netherlands Organization for Scientific Research (NWO) for a Veni grant. We also want to thank Prof. F. Lloret for stimulating discussions and J. M. Martínez-Agudo for the TGA measurements.

References

1 C. S. Mullins and V. L. Pecoraro, *Coord. Chem. Rev.*, 2008, **252**, 416.
2 G. Aromí and E. K. Brechin, *Struct. Bonding*, 2006, **122**, 1.
3 D. Gatteschi, R. Sessoli, and J. Villain, *Molecular Nanomagnets*, Oxford University Press, Oxford, 2006.
4 O. Kahn, *Molecular Magnetism*, Wiley-VCH, New York, 1993.
5 G. Aromí, S. M. J. Aubin, M. A. Bolcar, G. Christou, H. J. Eppley, K. Folting, D. N. Hendrickson, J. C. Huffman, R. C. Squire, H. L. Tsai, S. Wang and M. W. Wemple, *Polyhedron*, 1998, **17**, 3005.
6 G. Christou, *Polyhedron*, 2005, **24**, 2065.
7 C. J. Milios, R. Inglis, A. Vinslava, R. Bagai, W. Wernsdorfer, S. Parsons, S. P. Perlepes, G. Christou and E. K. Brechin, *J. Am. Chem. Soc.*, 2007, **129**, 12505 and ref. therein.
8 C. J. Milios, T. C. Stamatatos and S. P. Perlepes, *Polyhedron*, 2006, **25**, 134.
9 P. Chaudhuri, *Coord. Chem. Rev.*, 2003, **243**, 143.
10 M. A. Halcrow, *Dalton Trans.*, 2009, 2059.
11 J. Klingele, S. Dechert and F. Meyer, *Coord. Chem. Rev.*, 2009, **253**, 2698.
12 G. Aromí, E. Bouwman, E. Burzuri, C. Carbonera, J. Krzystek, F. Luis, C. Schlegel, J. van Slageren, S. Tanase and S. J. Teat, *Chem.–Eur. J.*, 2008, **14**, 11158.
13 G. Aromí, O. Roubeau, M. Helliwell, S. J. Teat and R. E. P. Winpenny, *Dalton Trans.*, 2003, 3436.
14 A. Bell, G. Aromí, S. J. Teat, W. Wernsdorfer and R. E. P. Winpenny, *Chem. Commun.*, 2005, 2808.
15 R. Boča, L. Dlhan, G. Mezei, T. Ortiz-Pérez, R. G. Raptis and J. Telser, *Inorg. Chem.*, 2003, **42**, 5801.
16 S. Demeshko, G. Leibeling, S. Dechert and F. Meyer, *Dalton Trans.*, 2006, 3458.
17 S. Tanase, G. Aromí, E. Bouwman, H. Kooijman, A. L. Spek and J. Reedijk, *Chem. Commun.*, 2005, 3147.

18 A. W. Addison and P. J. Burke, *J. Heterocycl. Chem.*, 1981, **18**, 803.
19 G. M. Sheldrick, *Program for Empirical Absorption Correction*, University of Göttingen, Germany, 1996.
20 P. T. Beurskens, G. Beurskens, M. Strumpel and C. E. Nordman, in *Patterson and Pattersons*, Clarendon Press, Oxford, 1987,p. 356.
21 A. J. M. Duisenberg, Reflections on area detectors, PhD Thesis, Utrecht, 1998.
22 A. J. M. Duisenberg, L. M. J. Kroon-Batenburg and A. M. M. Schreurs, *J. Appl. Crystallogr.*, 2003, **36**, 220.
23 P. T. Beurskens, G. Beurskens, W. P. Bosman, R. De Gelder, S. García-Granda, R. O. Gould, R. Israël, J. M. M. Smits and C. Smykalla, *The DIRDIF96. A computer program system for the crystal structure determination by Patterson methods and direct methods applied to difference structure factors*, Crystallography Laboratory, University of Nijmegen, Nijmegen, The Netherlands, 1996.
24 G. M. Sheldrick, *SHELXS-97, Program for Crystal Structures Determination*, University of Göttingen, Germany, Göttingen, 1997.
25 G. M. Sheldrick, *SHELXL-97, Program for Crystal Structure Refinement*, University of Göttingen, Germany, Göttingen, 1997.
26 A. L. Spek, *PLATON, A Multipurpose Crystallographic Tool*, Utrecht UniversityThe Netherlands, 2003.
27 M. Viciano-Chumillas, M. Marqués-Giménez, S. Tanase, M. Evangelisti, I. Mutikainen, M. Turpeinen, J. M. M. Smits, R. de Gelder, L. J. de Jongh and J. Reedijk, *J. Phys. Chem. C*, 2008, **112**, 20525–20534.
28 M. D. Godbole, O. Roubeau, A. M. Mills, H. Kooijman, A. L. Spek and E. Bouwman, *Inorg. Chem.*, 2006, **45**, 6713.
29 E. K. Brechin, M. Soler, G. Christou, M. Helliwell, S. J. Teat and W. Wernsdorfer, *Chem. Commun.*, 2003, 1276.
30 M. D. Godbole, O. Roubeau, R. Clérac, H. Kooijman, A. L. Spek and E. Bouwman, *Chem. Commun.*, 2005, 3715.
31 V. A. Grillo, M. J. Knapp, J. C. Bollinger, D. N. Hendrickson and G. Christou, *Angew. Chem., Int. Ed. Engl.*, 1996, **35**, 1818.
32 N. Hoshino, T. Ito, M. Nihei and H. Oshio, *Inorg. Chem. Commun.*, 2003, **6**, 377.
33 L. F. Jones, E. K. Brechin, D. Collison, J. Raftery and S. J. Teat, *Inorg. Chem.*, 2003, **42**, 6971.
34 E. Libby, K. Folting, C. J. Huffman, J. C. Huffman and G. Christou, *Inorg. Chem.*, 1993, **32**, 2549.
35 E. C. Sañudo, T. Cauchy, E. Ruiz, R. H. Laye, O. Roubeau, S. J. Teat and G. Aromí, *Inorg. Chem.*, 2007, **46**, 9045.
36 A. J. Tasiopoulos, W. Wernsdorfer, B. Moulton, M. J. Zaworotko and G. Christou, *J. Am. Chem. Soc.*, 2003, **125**, 15274.
37 H. L. Tsai, S. Y. Wang, K. Folting, W. E. Streib, D. N. Hendrickson and G. Christou, *J. Am. Chem. Soc.*, 1995, **117**, 2503.
38 S. Wang, H. L. Tsai, K. Folting, J. D. Martin, D. N. Hendrickson and G. Christou, *J. Chem. Soc., Chem. Commun.*, 1994, 671.
39 P. Baran, R. Boča, I. Chakraborty, J. Giapintzakis, R. Herchel, Q. Huang, J. E. McGrady, R. G. Raptis, Y. Sanakis and A. Simopoulos, *Inorg. Chem.*, 2008, **47**, 645.
40 R. G. Raptis, I. P. Georgakaki and D. C. R. Hockless, *Angew. Chem., Int. Ed.*, 1999, **38**, 1632.
41 L. Engelhardt, I. A. Gass, C. J. Milios, E. K. Brechin, M. Murrie, R. Prozorov, M. Vannette and M. Luban, *Phys. Rev. B: Condens. Matter Mater. Phys.*, 2007, **76**, 172406.
42 I. A. Gass, C. J. Milios, A. G. Whittaker, F. P. A. Fabiani, S. Parsons, M. Murrie, S. P. Perlepes and E. K. Brechin, *Inorg. Chem.*, 2006, **45**, 5281.
43 G. Vankalkeren, W. W. Schmidt and R. Block, *Physica B+C*, 1979, **97**, 315.
44 J. Krzystek, A. Ozarowski and J. Telser, *Coord. Chem. Rev.*, 2006, **250**, 2308.
45 G. Aromí, M. J. Knapp, J. P. Claude, J. C. Huffman, D. N. Hendrickson and G. Christou, *J. Am. Chem. Soc.*, 1999, **121**, 5489.
46 G. Aromí, J. P. Claude, M. J. Knapp, J. C. Huffman, D. N. Hendrickson and G. Christou, *J. Am. Chem. Soc.*, 1998, **120**, 2977.
47 N. E. Chakov, L. N. Zakharov, A. L. Rheingold, K. A. Abboud and G. Christou, *Inorg. Chem.*, 2005, **44**, 4555.
48 X. P. Xia, M. Verelst, J. C. Daran and J. P. Tuchagues, *J. Chem. Soc., Chem. Commun.*, 1995, 2155.
49 C. J. Milios, M. Manoli, G. Rajaraman, A. Mishra, L. E. Budd, F. White, S. Parsons, W. Wernsdorfer, G. Christou and E. K. Brechin, *Inorg. Chem.*, 2006, **45**, 6782.
50 C. J. Milios, C. P. Raptopoulou, A. Terzis, F. Lloret, R. Vicente, S. P. Perlepes and A. Escuer, *Angew. Chem., Int. Ed.*, 2004, **43**, 210.
51 C. J. Milios, A. Vinslava, W. Wernsdorfer, A. Prescimone, P. A. Wood, S. Parsons, S. P. Perlepes, G. Christou and E. K. Brechin, *J. Am. Chem. Soc.*, 2007, **129**, 6547.
52 C. P. Raptopoulou, A. K. Boudalis, K. N. Lazarou, V. Psycharis, N. Panopoulos, M. Fardis, G. Diamantopoulos, J. P. Tuchagues, A. Mari and G. Papavassiliou, *Polyhedron*, 2008, **27**, 3575.
53 C. Lampropoulos, K. A. Abboud, T. C. Stamatatos and G. Christou, *Inorg. Chem.*, 2009, **48**, 813.
54 M. Viciano-Chumillas, S. Tanase, I. Mutikainen, M. Turpeinen, L. J. de Jongh and J. Reedijk, *Inorg. Chem.*, 2008, **47**, 5919.
55 M. Viciano-Chumillas, S. Tanase, I. Mutikainen, U. Turpeinen, L. J. de Jongh and J. Reedijk, *Dalton Trans.*, 2009, 7445.

